

# Effect on Friction Reduction of Micro/Nano Hierarchical Patterns on Sapphire Wafers

Miru Kim<sup>1</sup>, Sang Min Lee<sup>2</sup>, Seung Jun Lee<sup>3</sup>, Yong Woo Kim<sup>4</sup>, Liang-Li<sup>1</sup>, and Deug Woo Lee<sup>5#</sup>

<sup>1</sup> Department of Nano Fusion Technology, Pusan National University, 1268-50, Samnangjin-ro, Samnangjin-eup, Miryang-si, Gyeongsangnam-do, 50463, South Korea

<sup>2</sup> Ulsan Center for Creative Economy & Innovation, 93, Daehak-ro, Nam-gu, Ulsan, 44610, South Korea

<sup>3</sup> Interdisciplinary Department for Innovative Manufacturing Engineering, Pusan National University, 2, Busandaehak-ro 63beon-gil, Geumjeong-gu, Busan, 46241, South Korea

<sup>4</sup> ERC of Innovative Technology on Advanced Forming, Pusan National University, 2, Busandaehak-ro 63beon-gil, Geumjeong-gu, Busan, 46241, South Korea

<sup>5</sup> Department of Nanomechanics Engineering, Pusan National University, 1268-50, Samnangjin-ro, Samnangjin-eup, Miryang-si, Gyeongsangnam-do, 50463, South Korea

# Corresponding Author | Email: dwoolee@pusan.ac.kr, TEL: +82-55-350-5281, FAX: +82-51-510-3129

KEYWORDS: Friction reduction, Micro/Nano hierarchical pattern, Coefficient of friction (COF), Stribeck curve, Laser machining, Abrasive air jet

*As well as the micro patterns, many functional surfaces exhibit micro/nano hierarchical patterns. Micro- and nano-patterned surfaces can be fabricated using various techniques including photolithography, electron-beams, and so on. However, these processes were developed for semiconductor fabrication and are not convenient for large-area applications. In this paper, we describe a manufacturing process for micro/nano hierarchical patterns using a laser and an abrasive air jet, whereby the laser is used to manufacture microscale patterns, and an abrasive air jet is applied to the micro-patterned surface to generate the nanoscale patterns. This method is a simple process that can be used to rapidly manufacture hierarchical patterns, making it suitable for large-area applications. We also developed a friction test system, which minimizes external vibrations and sample wear during the measurements. Our results showed that the coefficient of friction of the hierarchical patterns was 12% smaller than that of microscale patterns.*

Manuscript Received: June 17, 2016 | Revised: November 7, 2016 | Accepted: November 30, 2016

## NOMENCLATURE

$C_s$  = Coefficient of maximum static friction

$C_k = C_f$  = Coefficient of kinematic friction

$\mu$  = Dynamic viscosity

$U$  = Velocity in friction test

$P$  = Pressure in friction test

$O$  = Initial sapphire surface

$N$  = Nano patterned surface

$M$  = Micro patterned surface

$M+N$  = Micro/Nano hierarchical patterned surface

importance of efficiency in ‘traditional’ systems. For example, an important factor in energy efficiency is tribology, because reducing friction can save energy. There are many methods of reducing friction, such as surface coatings and the use of lubricants. Making a functional surface through mechanical machining can also improve energy efficiency by reducing friction. Friction characteristics depend on the properties of the surface. There are numerous surface treatments that aim to modify these surface properties, including methods to provide functionality by texturing micron-scale patterns.<sup>1</sup>

Micro-processing can be used to enhance the frictional and tribological properties of a surface. These techniques can be divided into mechanical, electrical and chemical methods.<sup>2</sup> Recently, complex micro/nano-scale patterns, as well as micro patterns, have attracted interest because of the functionality that can be created using this type of patterning. These functional surfaces can exhibit reduced friction, thus modifying the wear and lubrication characteristics. Most studies on functional surfaces that employ complex patterns have used biomimetic designs, whereby naturally occurring surfaces are mimicked.<sup>3</sup> For example, in the case of micro/nano hierarchical patterns, mosquitoes can remain on the surface of water without

## 1. Introduction

Recently, there have been many global concerns, such as energy shortages, resource depletion, and environmental pollution. For these and other reasons, there has been great interest in ‘green’ technologies; technologies to enhance energy efficiency have highlighted the

moving; high-magnification images of their legs indicate that this is due to the presence of micro/nano hierarchical patterns.<sup>4</sup> The applications of surfaces with such complex patterns include friction modification. In many mechanical systems, friction leads to wear. The use of micro- and nano-patterned surfaces can lead to reduced frictional forces, typically via storage of lubricant and binding to wear particles, and hydrodynamic effects can enhance the load-carrying capacity.<sup>5-9</sup>

There are several methods that can be used to manufacture micro/nano hierarchical patterns. The formation of micro patterns and nano patterns is typically carried out separately from other processes and requires complex manufacturing techniques. Lithography (such as that commonly used in semiconductor fabrication) can be applied to fabricate such patterns, as well as abrasive air jets and three-dimensional (3D) direct writing techniques that use high-energy electron beams or laser beams.<sup>10,11</sup> Furthermore, techniques such as electric discharge machining (EDM), electrochemical machining (ECM), and wire electrical discharge machining (WEDM) are commonly used to manufacture microscale patterns.

In this paper, we describe our research to reduce friction by providing texturing on a surface with micro/nano hierarchical patterns. We also investigated the manufacture of micro/nano hierarchical patterns manufactured on sapphire wafers. The process used to prepare these micro/nano hierarchical patterns employs laser machining to form the micro pattern, as well as abrasive air jet machining, whereby polishing particles are sprayed onto the surface to form the nano-scale pattern. This technique can be applied to large-area surfaces and rapid processing. Nano-Scale patterns are small and are often referred to as surface roughness. The frictional properties of the resulting surfaces were characterized. During this process, we shielded the samples from external vibrations, controlled the position, and measured the frictional force with various loads and transfer speeds to plot Stribeck curves.

## 2. Manufacturing of Micro/Nano Hierarchical Pattern

In our research, frictional force was measured to evaluate the functionality of micro/nano hierarchical patterns. Two different surfaces in relative motion were used to measure the drag generated while applying a normal force to the direction of motion. When a soft material is used repetitively on the same contact surface or point, abrasions may occur, which can lead to changes in the frictional forces. To maintain stability of the micro/nano hierarchical patterns, a sapphire sample with a Mohs hardness of 9 was used to minimize abrasion during the measurements. A 2-inch sapphire wafer (thickness: 0.4 mm), was lapped and cut into 20 mm × 20 mm samples; 10 mm × 10 mm micro patterns, nano patterns, and a micro/nano hierarchical pattern were manufactured at the center of these samples.

### 2.1 Manufacturing of Micro Pattern

Previous studies on the relationships between micro patterns and frictional forces focused on analysis of the influence of the shape, size and pitch of the patterns.<sup>12,13</sup> Methods for manufacturing patterns vary according to the materials used. In this research, we used laser machining, as it is suitable for large-area surfaces. Fig. 1 shows the laser equipment used to form micro patterns on sapphire wafers; Table

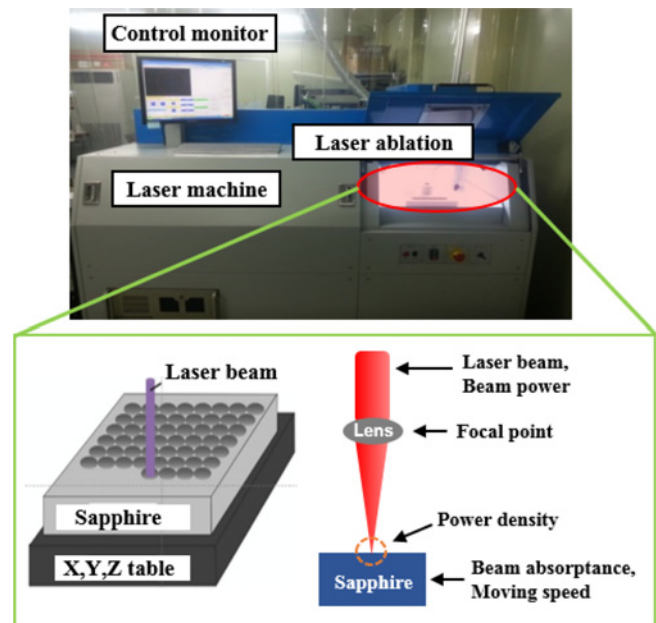


Fig. 1 Laser system for micro patterning on the sapphire

Table 1 Specifications of laser system

Mechanical axes	Stroke	X-Axis	150 mm
		Y-Axis	150 mm
		Z-Axis	80 mm
	Resolution	Linear motion	0.1 $\mu\text{m}$
Rotary motion		0.0001	
Optical axes	Scan field	70 × 70	
	Resolution	1.0 $\mu\text{m}$	
	Wavelength	355 nm	
Laser source	Average power	13 W	
	Repetition times	Max. 80 kHz	

Table 2 Micro patterning conditions

Pattern sizes (diameter, $\text{\O}$ × distance between center, $\mu\text{m}$ )		
Designed patterns	Manufactured patterns	Depth
$\text{\O} 30 \times (45, 60, 90)$	$\text{\O} 40 \times (60, 90, 150)$	100
$\text{\O} 60 \times (90, 120, 180)$	$\text{\O} 70 \times (90, 120, 180)$	200
$\text{\O} 90 \times (135, 180, 270)$	$\text{\O} 100 \times (135, 180, 270)$	300
$\text{\O} 120 \times (180, 240, 360)$	$\text{\O} 130 \times (180, 240, 360)$	200
$\text{\O} 150 \times (225, 300, 450)$	$\text{\O} 160 \times (225, 300, 450)$	200

1 lists the specifications of the equipment. The laser beam was focused to a triangular shape to penetrate into the surface of the sapphire wafer, allowing the circular conical micro patterns to be manufactured.

With the maximum laser power, the spot size was 20  $\mu\text{m}$  in diameter. Since exact positional control was difficult, the real manufactured patterns differed from the design value, with an error of  $\pm \text{\O} 10 \mu\text{m}$ . The micro patterns were manufactured on the sapphire sample according to the conditions listed in Table 2.

### 2.2 Manufacturing of Nano Pattern

The sample used in the frictional force experiments was a lapped sapphire wafer, with random nano patterns on the surface. The nano patterns were manufactured using an abrasive air jet. An abrasive air jet is a device for removing burrs generated by mechanical machining, and

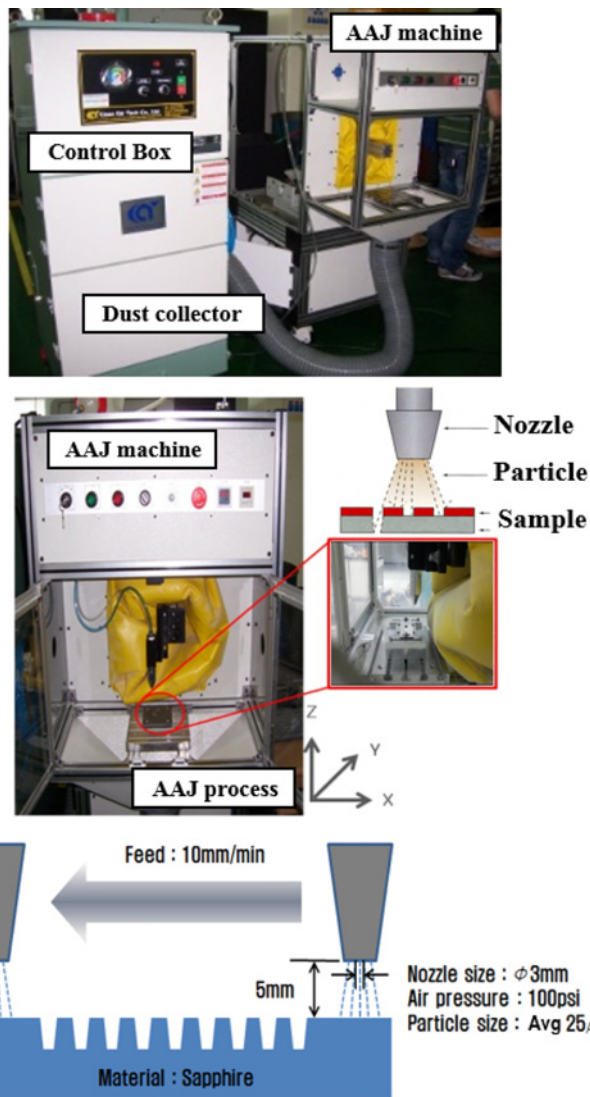


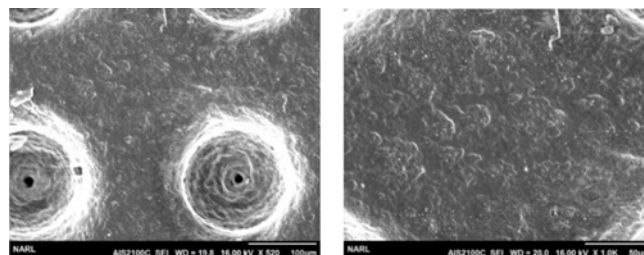
Fig. 2 Abrasive air jet system for nano patterning on the sapphire

Table 3 Abrasive air jet machining conditions

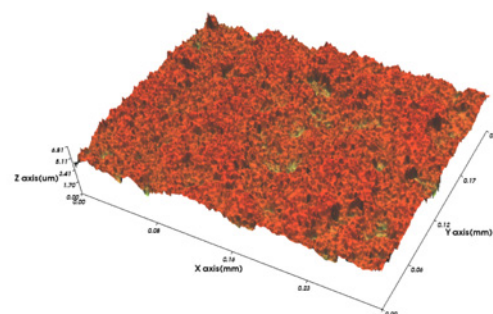
Powder material (size)	Al <sub>2</sub> O <sub>3</sub> (mean value: 25 μm)
Blasting pressure (psi)	100
Feed rate (mm/min)	10
Impact angle (°)	90
Mass flow rate (g/min)	90

involves spraying minute polishing particles. The size of these particles, as well as the air pressure and processing speed, were varied to control the nano patterns. Fig. 2 shows the abrasive air jet equipment, and Table 3 lists the processing conditions.

To investigate changes to the surface, the surface following processing with the abrasive air jet, were measured using a 3D non-contact surface profiler. Nano patterns were manufactured on the surface of the initial smooth sapphire sample, as well as on the lapped surface, where a micro pattern already existed. Although it was not possible to measure the nano patterns that were manufactured on the micro patterns, both patterns were manufactured using an identical abrasive air jet process, and it is reasonable to assume that the shape of the nano patterns was identical. Fig. 3 shows a scanning electron



(a) SEM image of surface after abrasive air jet process



(b) 3D profile: Ra= 350 nm, Rq= 450 nm

Fig. 3 SEM image and 3D profile of surface after abrasive air jet process

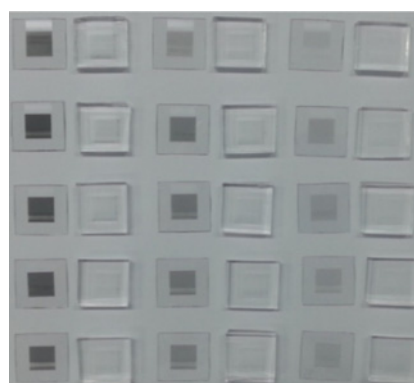


Fig. 4 Sapphire and PDMS samples including micro/nano pattern

microscope (SEM) image of the same sample surface that was measured using the 3D non-contact surface profiler.

### 2.3 Manufactured Micro/Nano Hierarchical Pattern

A 3D non-contact surface profiler is not useful for measuring the depth of a micro pattern because of the optical diffusion and reflection inside the pattern. Also, a contact-type surface profiler has a problem in that the center of the pattern cannot be accurately characterized. Measurements of the pattern depth were carried out by applying a polydimethylsiloxane (PDMS) coating to the sample, and transcribing it into a replica. Fig. 4 shows a sapphire sample processed with a 20 mm × 20 mm pattern, and the PDMS replica. Fig. 5 shows optical microscope images of part of the micro pattern manufactured on the sample, as well as the replica transcribed on PDMS. From left to right, we show the micro pattern manufactured using laser patterning, the micro/nano hierarchical pattern manufactured using laser patterning and the abrasive air jet, and the PDMS replica. The sample conditions and manufactured patterns are listed in Table 2.



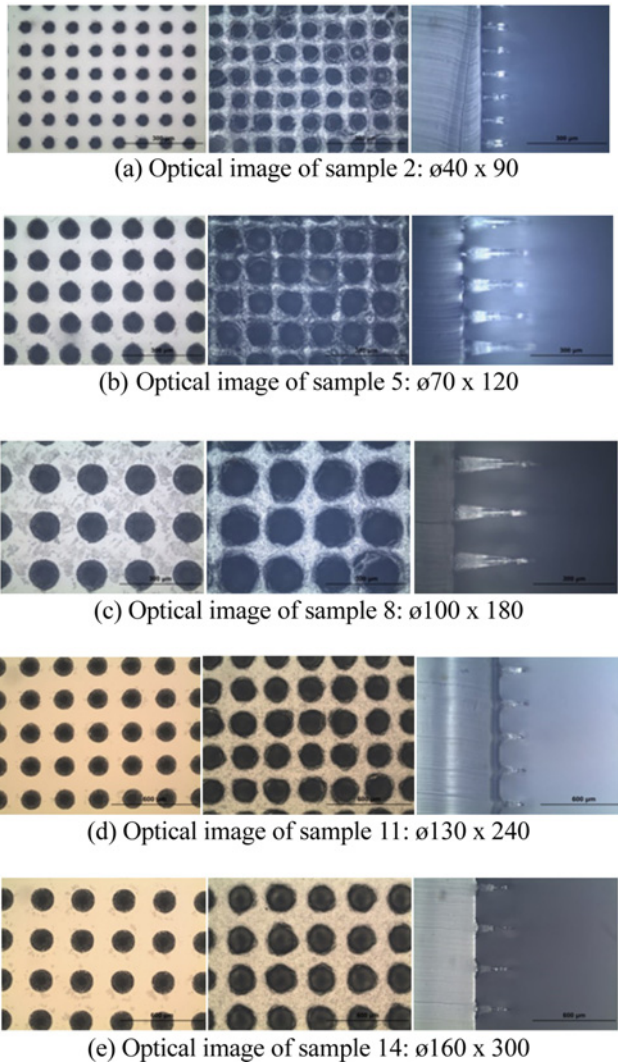


Fig. 5 Optical images of micro patterns, micro/nano hierarchical patterns and the PDMS replica

### 3. Experimental Process

#### 3.1 Configuration of the Friction Test Equipment

A tribometer measures friction and wear on a sample in rotary motion based on the frictional force caused by a point contact; however, the results may be insufficient for characterizing surface contact with higher dimensionality. The tribometer should rotate for a long period of time following loading; therefore, wear will occur at the contact point. Because the results are obtained by averaging data, which may occur throughout the measurement, it is difficult to characterize accurately the frictional force on the initial sample surface.

The frictional force on the sample depends on the micro pattern, and localized pressure caused by the size of the ball may lead to wear. This also makes it difficult for the ball to remain at the center of the pattern. Therefore, to enable surface contact measurements of the frictional forces, and to minimize wear to the nano patterns, we developed a new system to measure the frictional force over a single cycle.

Fig. 6 shows the friction test system used for measuring the frictional force. Translation in the x-axis was enabled using an air guideway, and vibration was minimized using an anti-vibration pad.

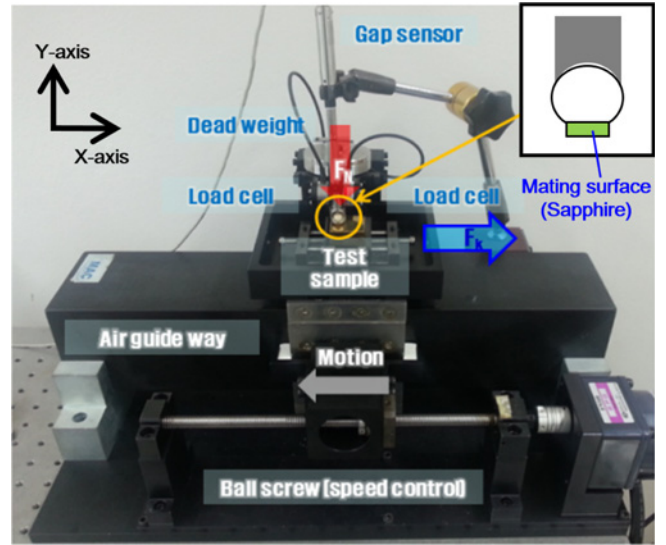


Fig. 6 Image of manufactured friction test system

Table 4 Dry friction test conditions for verification

Motion	1 cycle (One Way)
Stroke (mm)	± 20
Load (N)	6.6, 8.6, 10.6
Feed rate (mm/min)	10

Table 5 Specifications of tribometer (UFW200)

Rotation module	Linear reciprocation module
- Upper pin or ball specimen: Stationary or automatic positioning on disc radius 1 to 1,000 rpm	- Upper pin/Ball/Block - Distance 0 - 25 mm
- Automatic radial positioning: Range 15 mm, Resolution 0.1 mm	- Reciprocating frequency 0.1 - 20 Hz - Reciprocating stroke 0.1 - 25 mm

Table 6 Compared results of coefficients of friction for verification

Tribometer model	Developed friction test system	UFW200	
Coefficient of maximum static friction ( $C_s$ )	6.6 N	0.108	0.098
	8.6 N	0.103	0.101
	10.6 N	0.093	0.097
Coefficient of kinematic friction ( $C_k$ )	6.6 N	0.091	0.081
	8.6 N	0.089	0.084
	10.6 N	0.088	0.083

Table 7 Friction test conditions with lubricant

Motion	1 cycle (One Way)
Stroke (mm)	± 20
Load (N)	1.6, 2.6, 4.6, 6.6, 8.6, 10.6
Feed rate (mm/min)	10

Installing load cells on the left and right enabled measurement of the frictional force opposing translation. The load was applied to the y-axis, and could be controlled. The ball on the tip of the stylus cut vertically, and a sapphire surface was attached for the mating surface. The sapphire sample was 0.4 mm thick and was cut to 2 mm × 2 mm.

The reliability of the data was assessed prior to the experiments. We compared the coefficient of friction of the friction test system developed

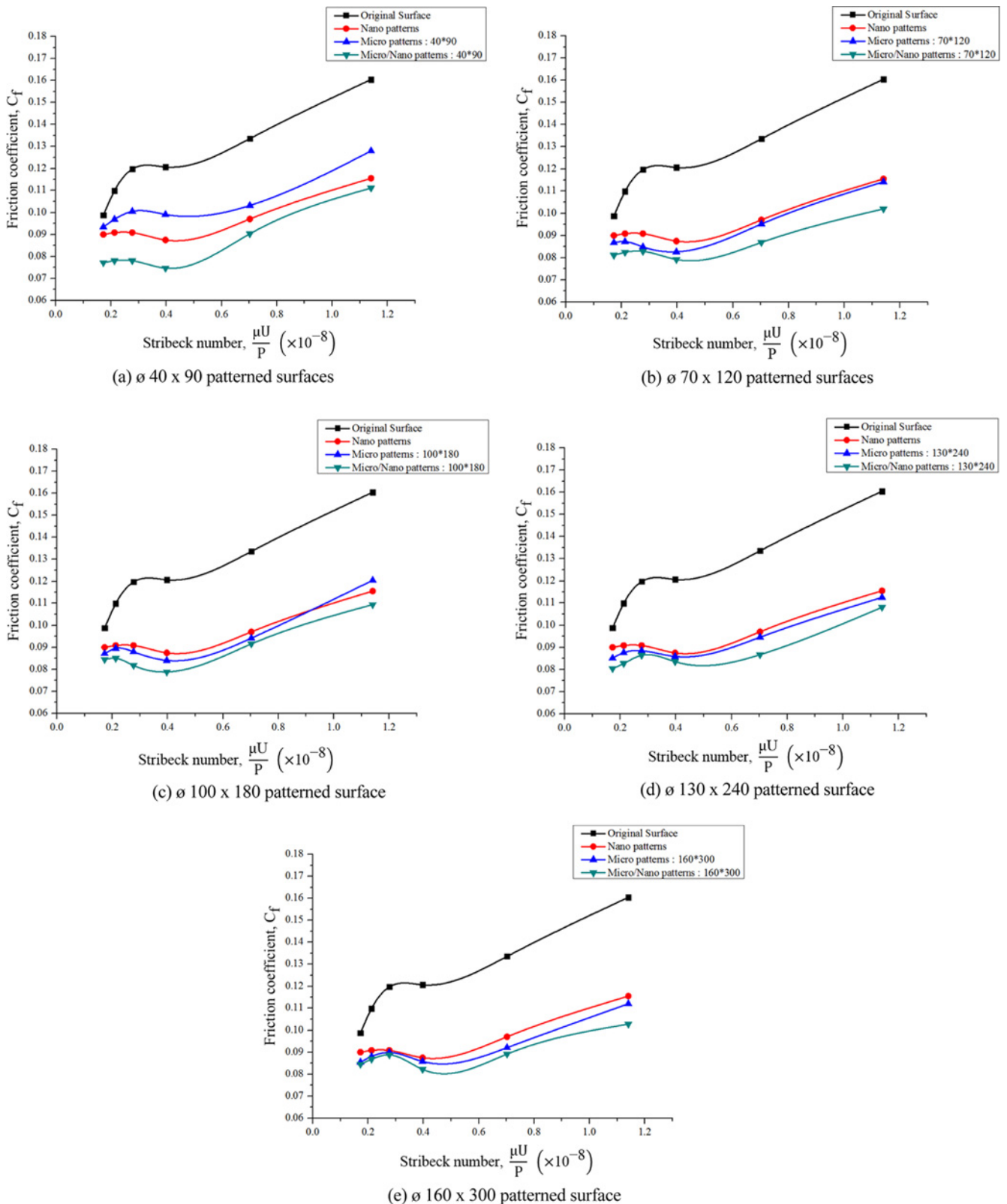


Fig. 7 Stribeck curves of friction tests under lubricating and surface types

here and a commercial tribometer. The initial sapphire sample was used to measure the frictional force. An identical sample was used as the mating surface to minimize wear generated during measurement. Dry friction analysis was carried out to measure the friction coefficient. The coefficient of maximum static friction of the sapphire-sapphire interface was 0.1,

according to the manufacturer of the sapphire wafer and other references.<sup>14,15</sup> Table 4 lists the experimental conditions used during the friction experiment. The actual load was 0.6 N greater than the applied load, to account for the mass of the stylus (Fig. 6). The minimum applied load was 5 N, and we investigated loads of 6.6 N, 8.6 N, and 10.6 N (Table 4).

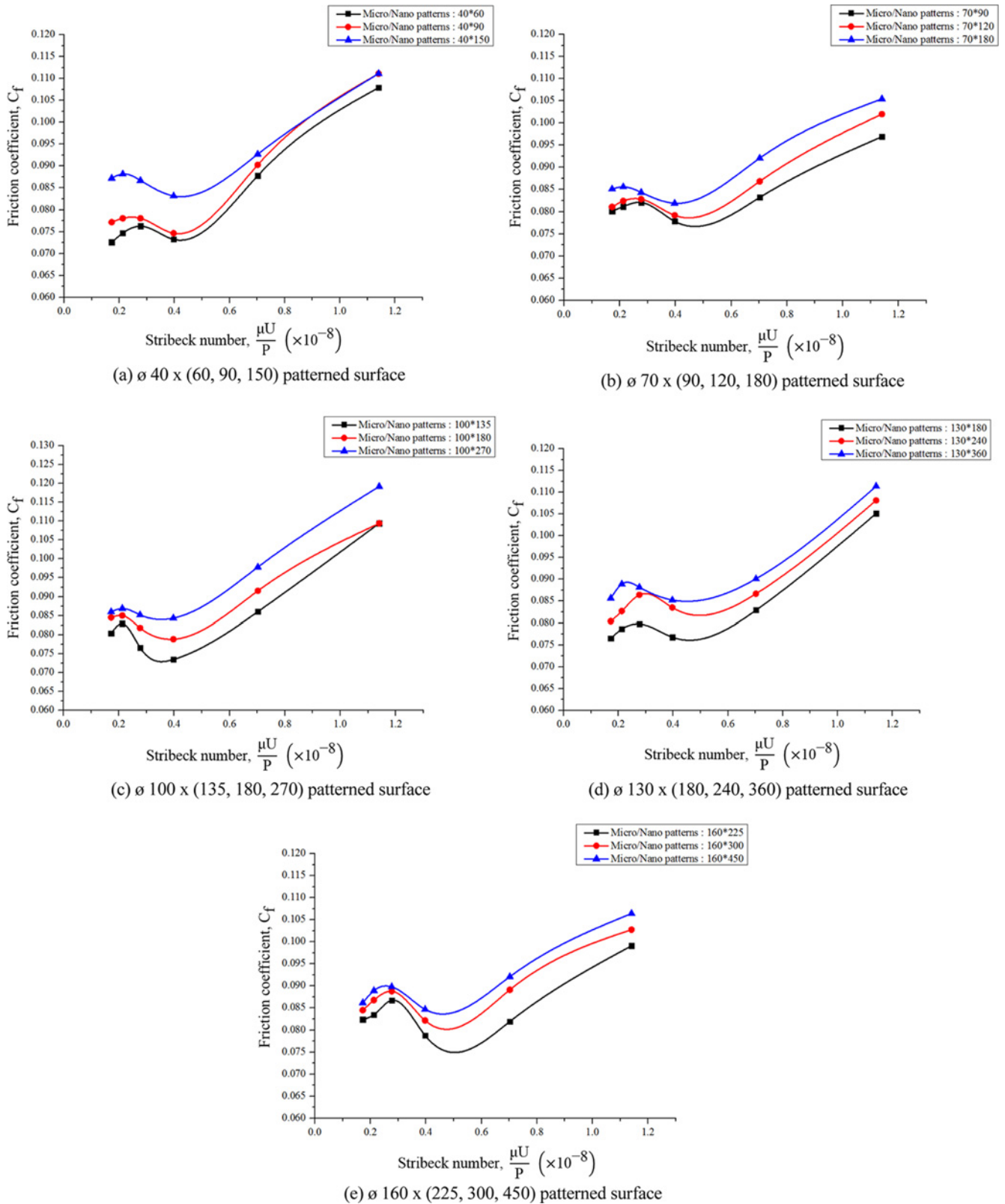


Fig. 8 Stribeck curves of friction tests under lubricating and variations distance of micro patterns

Table 5 lists the specifications of the commercial tribometer (NEOPLUS’s UFW200).<sup>16</sup> Table 6 lists the measured coefficients of friction characterized in identical conditions, using the friction test system developed in this research and the commercial tribometer. The coefficient of maximum static friction,  $C_s$ , was 0.1, giving an error of  $\pm 5\%$ .

### 3.2 Friction Test of Each Pattern Types

The four types of sapphire surface (the initial sapphire surface, the micro-patterned surface, the nano-patterned surface with applied surface roughness and the micro/nano hierarchical pattern) were used in the surface contact frictional experiments, and the frictional forces

were measured using a 2 mm × 2 mm sapphire sample as the mating surface. To investigate the effects of the patterning, the coefficient of friction was measured for a single cycle, along a straight line. To include the entire pattern, the measurement length was 20 mm, and the transfer speed was 10 mm/min. Table 7 lists the conditions during the measurements. In all experiments, a lubricant was applied to minimize wear; we used a commercially available oil with a viscosity of 27.44 cP.

#### 4. Results and Discussions

To compare frictional forces between micro-patterned and nano-patterned surfaces, the surfaces of the samples were classified into four types: the initial smooth sapphire surface (original surface), micro-patterned surfaces (micro patterns), nano-patterned surface (nano patterns), and surfaces with micro/nano hierarchical patterns (micro/nano patterns). After adding lubricant, experiments were carried out according to the conditions listed in Table 7, and the coefficients of kinematic friction were measured ( $C_k = C_f$ ). The number of data points was 1,080 (4 surface types × 15 samples each × 6 loads × 3 repetitions of each measurement). Fig. 7 shows the resulting Stribeck curves on different surface types. The frictional force was measured for different surface types manufactured using the conditions listed in Table 2 and Fig. 8 shows a comparison of the Stribeck curves according to different sized micro/nano patterns, which was derived by the distance between micro patterns. In Figs. 7 and 8, the Stribeck number is a dimensionless number given by  $(\mu \times U) / P$ , where  $\mu$  is the lubricant dynamic viscosity,  $U$  is the velocity (= feed rate in Table 7), and  $P$  is the contact pressure in the friction test.<sup>17,18</sup>

Table 8 lists the coefficients of friction for the four types of surface. The coefficient of friction was largest for the initial sapphire surface (O), followed by the nano-patterned surface (N) and the micro-patterned surface (M). The coefficient of friction was smallest for the micro/nano hierarchical patterned (M+N) surface.

The nano-patterned surface has a surface roughness governed by its nano patterns. Compared with the initial sapphire surface, the coefficient of friction of the nano-patterned surface is attributable to the low contact area due to the nano patterns between the mating surfaces.<sup>19</sup> Thus, the nano-patterned surface showed a lower coefficient of friction than the initial sapphire surface. The micro-patterned surface has dimple patterns. It was considered that the hydrodynamic pressure, caused by fluid flow changes, increased locally near the dimple patterns and the load-carrying capacity of lubricant film was improved by the shape of the dimple patterns.<sup>20,21</sup> The micro/nano hierarchical-patterned surface had both the effects of the nano patterns, with a low contact area, and that due to the micro patterns, with hydrodynamic pressure and load-supporting capacity. Consequently, the micro/nano hierarchical-patterned surface showed the lowest coefficient of friction.

This provides some evidence of the functionality of the micro/nano hierarchical patterns; however, when the distance of the micro patterns increased to more than three times the size of the features of the pattern, the frictional force for the micro-patterned surface was greater than that for the nano-patterned surface. This is attributed to

Table 8 Comparison of coefficients of friction according to surface types (Surface types: O, M, N, M+N)

Pattern sizes, $\varnothing$ ( $\mu\text{m}$ )	Pattern distance ( $\mu\text{m}$ )	Coefficients of friction (surface conditions)
40 (Designed size : 30)	60	O > N > M > M+N
	90	O > M > N > M+N
	150	O > M > N > M+N
70 (Designed size : 60)	90	O > N > M > M+N
	120	O > N > M > M+N
	180	O > M > N > M+N
100 (Designed size : 90)	135	O > N > M > M+N
	180	O > N > M > M+N
	270	O > M > N > M+N
130 (Designed size : 120)	180	O > N > M > M+N
	240	O > N > M > M+N
	360	O > M > N > M+N
160 (Designed size : 150)	225	O > N > M > M+N
	300	O > N > M > M+N
	450	O > M > N > M+N

Table 9 Comparison of coefficients of friction according to distance of the micro patterns (Surface types : O, M, N, M+N)

Surface conditions	Pattern sizes, $\varnothing$ ( $\mu\text{m}$ )	Coefficients of friction (Patterns conditions)
M	40 (Designed size : 30)	150 > 90 > 60
M+N		150 > 90 > 60
M	70 (Designed size : 60)	180 > 120 > 90
M+N		180 > 120 > 90
M	100 (Designed size : 90)	270 > 180 > 135
M+N		270 > 180 > 135
M	130 (Designed size : 120)	360 > 240 > 180
M+N		360 > 240 > 180
M	160 (Designed size : 150)	450 > 300 > 225
M+N		450 > 300 > 225

insufficient force supporting the load between the corresponding surfaces.

Table 9 shows the ranges of the coefficients of friction according to distance between micro patterns. With the micro-patterned surfaces (M) and the micro/nano hierarchical-patterned surfaces (M+N), the coefficient of friction increased as the distance of the micro patterns increased. For a given distance, the coefficient of friction for the micro/nano hierarchical-patterned surface was - 12% smaller than that of the micro-patterned surface.

In any pattern on a surface having a friction-reducing effect, durability is an important factor. If the durability is poor, the friction-reducing effect will decline as the pattern becomes broken and scratched. However, the surface material used here was sapphire, which has high hardness and wear resistance. In the case of a micro/nano hierarchical pattern or nano pattern, it may show less durability than the micro-patterned surface alone and the initial sapphire surface due to its rough surface, but the coefficient of friction will be lower as a functional benefit. After 1080 repetitions of the friction tests in this study, there was no evidence of degradation in the pattern shapes. Thus, all of the patterns on sapphire, including the micro/nano hierarchical pattern, showed good long-term durability.

## 5. Conclusions

We fabricated micro/nano hierarchical-patterned surfaces on sapphire wafers using laser machining and abrasive air jet machining, and measured the frictional properties of the resulting surfaces. The major results of this work can be summarized as follows:

(1) Laser machining and an abrasive air jet were used to form micro/nano hierarchical-patterned surfaces on sapphire and were suitable for large-area manufacturing. Circular conical patterns were manufactured with a diameter of 40 - 160  $\mu\text{m}$ . Using the abrasive air jet, a micro/nano hierarchical pattern was prepared with a surface roughness of  $R_q = 450$  nm. The micro/nano hierarchical pattern was transcribed onto a PDMS replica to measure the depth of the patterns.

(2) Time-averaged rotary motion or reciprocating motion can be used to measure the coefficient of friction; however, this causes wear, changing the properties of the surface during the experiment. Instead, we developed a friction test system: we used an x-y linear translation set-up to minimize wear to the surface, to measure the frictional properties. An air guide was used to minimize external vibration.

(3) The surfaces of the sapphire samples were classified into four types. The coefficient of friction was largest for the initial smooth sapphire surface (O), followed by the nano-patterned surface (N), the micro-patterned surface (M), and the micro/nano hierarchical-patterned (M+N) surface. Thus, the micro/nano hierarchical pattern was effective in reducing friction. However, when the distance between the micro patterns increased to more than three times the size of the micro pattern, the frictional force for the micro-patterned surface was greater than that for the nano-patterned surface. As the distance of both the micro and micro/nano hierarchical patterns increased, so did the coefficient of friction. The coefficient of friction of the micro/nano hierarchical patterned surfaces (M+N) was - 12% lower than that of the micro-patterned surfaces (M).

## ACKNOWLEDGEMENT

This work was supported by "Development of ICT-based smart machine tools and flexible automation systems" of the Ministry of Trade, Industry and Energy (MOTIE), Korea (Grant No. 10060188) and "Development of Core Technologies for High-Reliability Vertical Machining Centers" of the Ministry of Trade, Industry and Energy (MOTIE), Korea [Grant No. 10063361].

## REFERENCES

- Kim, J., Je, T. J., Cho, S. H., Jeon, E. C., and Whang, K. H., "Micro-Cutting with Diamond Tool Micro-Patterned by Femtosecond Laser," *Int. J. Precis. Eng. Manuf.*, Vol. 15, No. 6, pp. 1081-1085, 2014.
- Kurniawan, R. and Ko, T. J., "Friction Reduction on Cylindrical Surfaces by Texturing with a Piezoelectric Actuated Tool Holder," *Int. J. Precis. Eng. Manuf.*, Vol. 16, No. 5, pp. 861-868, 2015.
- Tsipenyuk, A. and Varenberg, M., "Use of Biomimetic Hexagonal Surface Texture in Friction Against Lubricated Skin." *Journal of the Royal Society Interface* Vol. 11, No. 94, Paper No. 20140113, 2014.
- Wu, C.W., Kong, X. Q., and Wu, D., "Micronanostructures of the Scales on a Mosquito's Legs and their Role in Weight Support," *Physical Review E*, Vol. 76, No. 1, Paper No. 017301, 2007.
- Rykaczewski, K., Paxson, A. T., Staymates, M., Walker, M. L., Sun, X., et al., "Dropwise Condensation of Low Surface Tension Fluids on Omniphobic Surfaces," *Scientific Reports*, Vol. 4, No. 4158, 2014.
- Borghi, A., Gualtieri, E., Marchetto, D., Moretti, L., and Valeri, S., "Tribological Effects of Surface Texturing on Nitriding Steel for High-Performance Engine Applications," *Wear*, Vol. 265, No. 7, pp. 1046-1051, 2008.
- Wanga, X., Katoa, K., Adachia, K., and Aizawab, K., "Loads Carrying Capacity Map for the Surface Texture Design of SiC Thrust Bearing Sliding in Water," *Tribology International*, Vol. 36, No. 3, pp. 189-197, 2003.
- Hao, L., Meng, Y., and Chen, C., "Experimental Investigation on Effects of Surface Texturing on Lubrication of Initial Line Contacts," *Lubrication Science*, Vol. 26, No. 5, pp. 363-373, 2014.
- Myshkin, N. K. and Grigoriev, A. Y., "Morphology: Texture, Shape, and Color of Friction Surfaces and Wear Debris in Tribodiagnosis Problems," *Journal of Friction and Wear*, Vol. 29, No. 3, pp. 192-199, 2008.
- Shao, J., Ding, Y., Wang, W., Mei, X., Zhai, H., et al., "Generation of Fully-Covering Hierarchical Micro-Nano-Structures by Nanoimprinting and Modified Laser Swelling," *Small*, Vol. 10, No. 13, pp. 2595-2601, 2014.
- Röhrig, M., Thiel, M., Worgull, M., and Hölscher, H., "3D Direct Laser Writing of Nano- and Microstructured Hierarchical Gecko-Mimicking Surfaces," *Small*, Vol. 8, No. 19, pp. 3009-3015, 2012.
- Ajayi, O. O., Greco, A. C., Erck, R. A., and Frenske, G. R., "Surface Texturing for Friction Control," *Argonne National Laboratory*, pp. 1-13, 2010.
- Wang, W.-Z., Huang, Z., Shen, D., Kong, L., and Li, S., "The Effect of Triangle-Shaped Surface Textures on the Performance of the Lubricated Point-Contacts," *Journal of Tribology*, Vol. 135, No. 2, pp. 1-11, 2013.
- Tang, H., Li, H., and Xu, J., "Growth and Development of Sapphire Crystal for LED Applications," *INTECH Open Science and Open Minds*, Chap. 10, pp. 307-333, 2013.
- Precision Sapphire Technologies, "Our Products-Sapphire Physical properties," <http://www.sapphire.lt/sapphire> (Accessed 23 December 2016)
- Neoplus, "Product-Tribology System Friction & Wear Test System-UFW200," [http://i-neoplus.co.kr/02\\_product/tribology-equipment.php](http://i-neoplus.co.kr/02_product/tribology-equipment.php) (Accessed 23 December 2016)



17. Stribeck, R. and Cutaway, C., "Generating a Stribeck Curve in a Reciprocating Test (HFRR/SRV-type test)," [https://www.bruker.com/fileadmin/user\\_upload/8-PDF-Docs/SurfaceAnalysis/TMT/Application\\_Notes/AN1004\\_RevA2\\_Generating\\_a\\_Stribeck\\_Curve\\_in\\_a\\_Reciprocating\\_Test-AppNote.pdf](https://www.bruker.com/fileadmin/user_upload/8-PDF-Docs/SurfaceAnalysis/TMT/Application_Notes/AN1004_RevA2_Generating_a_Stribeck_Curve_in_a_Reciprocating_Test-AppNote.pdf) (Accessed 23 December 2016)
18. Etsion, I., Halperin, G., and Becker, E., "The Effect of Various Surface Treatments on Piston Pin Scuffing Resistance," *Wear*, Vol. 261, No. 7, pp. 785-791, 2006.
19. Elleuch, R., Elleuch, K., Abdelounis, H. B., and Zahouani, H., "Surface Roughness Effect on Friction Behaviour of Elastomeric Material," *Materials Science and Engineering A*, Vol. 465, No. 1, pp. 8-12, 2007.
20. Nakano, M., Korenaga, A., Korenaga, A., Miyake, K., Murakami, T., et al., "Applying Micro-Texture to Cast Iron Surfaces to Reduce the Friction Coefficient Under Lubricated Conditions," *Tribology Letters*, Vol. 28, No. 2, pp. 131-137, 2007.
21. Yu, H., Wang, X., and Zhou, F., "Geometric Shape Effects of Surface Texture on the Generation of Hydrodynamic Pressure Between Conformal Contacting Surfaces," *Tribology Letters*, Vol. 37, No. 2, pp. 123-130, 2010.